Applied Catalysis B: Environmental 113–114 (2012) 2–10

Contents lists available at ScienceDirect

Applied Catalysis B: Environmental

journal homepage: www.elsevier.com/locate/apcatb

Methanation of CO_2: Further insight into the mechanism over $Rh/\gamma\text{-}Al_2O_3$ catalyst

Antoine Beuls [a], Colas Swalus [a], Marc Jacquemin [a], George Heyen [b], Alejandro Karelovic [a,*], Patricio Ruiz [a]

[a] Institute of Condensed Matter and Nanosciences (IMCN), Division Molecules, Solids and Reactivity (MOST), Université Catholique de Louvain, Croix du Sud, 2/17, 1348 Louvain la Neuve, Belgium
[b] LASSC, Department of Applied Chemistry, Faculty of Applied Sciences, University of Liege, Belgium

ARTICLE INFO

Article history:
Available online 5 March 2011

Keywords:
Carbon dioxide
Mechanism methanation
Hydrogenation
Influence carbon monoxide oxygen

ABSTRACT

The methanation of CO_2 was performed on $Rh/\gamma\text{-}Al_2O_3$ catalyst at temperatures between 50 and 150 °C at 2 bar of pressure in a pulse reactor. Experiments confirm the formation of methane at low temperature and pressure. The formation of formiate species during the adsorption of CO_2 can be excluded. After reaction with CO_2, the catalyst is oxidized. Oxidation is not observed in the presence of CO. The CO_2 is adsorbed dissociatively, forming CO (ads) and O (ads). Gem-dicarbonyl $Rh(CO)_2$ species are more reactive than the Rh–CO linear species. The type of adsorbed species depends on the Rh oxidation state. The formation of methane by hydrogenation of CO_2 and CO is carried out with 100% selectivity. The activation energy for the hydrogenation of CO_2 and CO is lower than values presented in the literature which have been obtained at higher temperature. In the presence of CO_2 and CO, the reaction of methanation of CO_2 seems to be inhibited by CO. When oxygen is added in low amount in the reactant gas feed, a positive effect on methanation is observed. When the amount of oxygen is too high, oxygen has a negative effect. These results are in agreement with thermodynamics equilibrium calculations, except when O_2 is present, confirming the importance of kinetic effects in the reaction. These results open new perspectives of application of catalysis, in order to recycle CO_2 in the presence of H_2.

1. Introduction

The reduction of CO_2 emissions requires implementation of preventive actions, higher efficiency processes, development of new technological systems and viable alternatives to the conventional use of fossil hydrocarbons, and at the same time, supplementary curative measures [1,2]. The increase of greenhouse gases in the atmosphere (mainly CO_2) has made the transformation of CO_2 into useful chemicals and fuels important areas of research. Efforts are made nowadays to implement curative actions aiming at the capture and sequestration of CO_2 [3,4], however a hard work and further fundamental studies are necessary to master this complex technology [3,4]. Technologies including utilization of CO_2 will be a key response strategy for protecting the environment. The great handicap to develop such technologies is the high stability of CO_2. Its activation imposes a scientific challenge. New concepts and fundamental advances are highly necessary to promote emergent technologies using CO_2. Previous experiments performed in our laboratory give evidence that at (low) room temperature and at (low) atmospheric pressure, it is possible to obtain methane when putting CO_2 and H_2 in the presence of an adequate catalyst [5,6]. The formation of CH_4 under these conditions is an important breakthrough in the knowledge of the role and in the use of CO_2 and gives valuable insight into the selectivity. However the formation of methane at room temperature appeared contradictory compared with thermodynamic calculations when the reactivity of CO_2 is considered. Indeed, it is estimated that not more than 2% of $CO_{2(g)}$ transform into $CO_{(g)}$ and $O_{2(g)}$ at 2000 °C. Then, at temperatures low enough (<200 °C), CO_2 is considered as completely inert. To explain the formation of methane at such a low temperature, we have demonstrated experimentally that the first step in the mechanism by which this reaction occurs is due to the dissociation of CO_2 on the surface of the catalysts ($CO_{2(g)} = CO_{(adsorbed)} + O_{(adsorbed)}$) [6]. The extent of this reaction is low but it is thermodynamically favourable [7,8]. In a second step, this dissociated species reacts with H_2 to produce methane.

In this work, further insights into the mechanism of methanation are given. CO_2 and CO hydrogenations are compared. The influence of CO in the feed in the hydrogenation of CO_2, the influence of oxygen in the feed in the hydrogenation of CO_2 and CO and the influence of the temperature in the methanation of CO_2 and CO is studied. The results confirm the mechanism suggested previously and give important information to improve the CO_2 methanation process.

* Corresponding author. Tel.: +32 10 47 3651; fax: +32 10 47 3649.
E-mail addresses: alejandro.karelovic@student.uclouvain.be, akarelov@gmail.com (A. Karelovic).

0926-3373/$ – see front matter © 2011 Elsevier B.V. All rights reserved.
doi:10.1016/j.apcatb.2011.02.033

2. Experimental

2.1. Catalyst preparation

The catalyst (Rh (1 wt.%)/γ-Al_2O_3) was prepared by wet impregnation of alumina with a solution of $(NH_4)_3RhCl_6{\cdot}3H_2O$ (Across, 195510010). 10 g of γ-Al_2O_3 (Alfa Aesar, 39812) were dipped in 200 ml of distilled water. The rhodium precursor was added to obtain 1% by weight. The solution was mixed at 60 °C for 18 h under magnetic stirring. After evaporation of the solvent under reduced pressure in a rotavapor, the catalyst was dried at 110 °C for 12 h and calcined at 450 °C for 2 h in a furnace under static air.

2.2. Catalytic tests

The catalyst was sieved and selected in the 200–315 μm fraction. 150 mg of catalyst were introduced on the frit of a quartz reactor of 8 mm internal diameter located inside an electrically heated furnace. The temperature was checked with a thermocouple located inside a quartz thermowell fixed into the catalytic bed. Pressure was 100 and 300 kPa.

The first step of the catalytic test was the reduction of the solid under a flow of pure H_2 (Praxair, 4.8) at 350 °C for 1 h and cooled down until the temperature of the catalytic test under He (Praxair, 4.8), namely 125 °C. Then a pulse (volume = 1.02 cm^3) of CO_2 (Praxair, 4.8) or CO (Praxair, 4.8) was introduced in the reactor using H_2 as a carrier. Experiments were also performed introducing simultaneously pulses of mixtures of CO_2 + CO or mixtures of CO_2 + O_2 (Praxair, 2.2) or CO + O_2. In some cases the temperature was varied between 50 °C and 200 °C. Mass of reactant and products were monitored by a quadrupole mass spectrometer (Balzers QMS 200). Data were analyzed using the Balzers Alters Quadstar 422 Measurement interface. The mass fragments of He, H_2, H_2O, CO, CO_2, CH_4, C_2–C_3 hydrocarbons and C_1–C_2 oxygenated hydrocarbons were studied. The integration of peaks was performed using the Origin Pro 8 software. Reaction rates were calculated from de amount of methane formed divided by the mass of catalyst and time of reaction.

2.3. Characterization

Catalysts were characterized by elemental analysis, N_2 adsorption/desorption, XRD, XPS, CO_2 and H_2 chemisorption and in situ DRIFTS.

The chemical composition of the catalyst was determined by inductively coupled plasma atomic emission spectroscopy (ICP-AES) on an Iris Advantage equipment from Jarrel Ash Corporation. The samples were first brought into solution by alkali oxidative fusing NaOH/Na_2O_2 and subsequent dissolution with diluted HCl.

Textural analysis of the catalyst was carried out on a Micromeritics ASAP 2000/2010 equipment using N_2 (Praxair, 4.8) adsorption/desorption at liquid N_2 temperature, working with P/P_0 pressures in the range of 10^{-2} to 1.0. Before the measurements, 150 mg of the samples were degassed at 423 K overnight under a 50 mTorr vacuum. BET and Barret Joyner and Halenda equations were used to determine surface area, porous volume and pores size distribution.

X-ray diffraction (XRD) analyses were performed on the fresh catalyst on a Siemens D5000 diffractometer using the Kα radiation of Cu (λ = 1.5418 Å). The 2θ range was scanned between 10 and 90° by steps of 0.02° with an acquisition time of 2 s at each step. Identification of the phases was carried out using the ICDD-JCPDS database.

Surface characterization of the fresh catalyst, of the catalyst after reduction and after the catalytic test, was done by X-ray photoelectron spectroscopy (XPS) measurements on a Kratos Axis Ultra spectrometer (Kratos Analytical – Manchester – UK) equipped with a monochromatised aluminium X-ray source (powered at 10 mA and 15 kV). The samples powders were pressed into small stainless steel troughs mounted on a multi specimen holder. The pressure in the analysis chamber was around 10^{-6} Pa. The angle between the normal to the sample surface and the lens was 55°. The analyzed area was 700 μm × 300 μm. The pass energy of the hemispherical analyzer was set at 40 eV. Charge stabilization was achieved by using the Kratos Axis device. The electron source was operated at a filament current of 1.8 A and a bias of −1.1 eV. The following sequence of spectra was recorded: survey spectrum, C 1s, O 1s, Al 2p and Rh 3d and C 1s again to check the stability of charge compensation as a function of time and the absence of degradation of the sample during the analyses. The binding energy (BE) values were referred to the C-(C,H) component of the C 1s peak fixed at 284.8 eV. The spectra were decomposed with the CasaXPS program (Casa Software Ltd., UK) with a Gaussian/Lorentzian (70/30) product function. Molar fractions were calculated using peak areas normalised on the basis of acquisition parameters, sensitivity factors and transmission factors provided by the manufacturer.

The CO_2 chemisorption measurements were performed on a Micromeritics ASAP2010Chemi apparatus. The U-shaped sample tube containing about 150 mg of the catalyst was first flushed under a H_2 flow at 350 °C for 1 h for reducing the catalyst and under He flow at 350 °C for 1 h for the non-reduced catalyst and then flushed with a He flow at 25 °C for 2 h. Finally the samples were evacuated at 25 °C for 2 h under a residual pressure of <5 μmHg. A first CO_2 adsorption isotherm was taken at 25 °C. Then the sample was evacuated at the same temperature and a second CO_2 adsorption isotherm was measured. The difference between the two isotherms corresponds to the amount of carbon dioxide chemisorbed on the samples at 25 °C. The results were expressed in terms of cm^3 of chemisorbed CO_2 per gram of catalyst.

Dispersion of Rh on γ-Al_2O_3 was determined by hydrogen chemisorption. Experiments were conducted at 35 °C using a Micromeritics ASAP2010Chemi apparatus. The sample (150 mg) was first degassed under vacuum down to <5 μmHg. Then it was reduced at 350 °C under a pure flow of hydrogen (Praxair, 5.0) for 1 h and then flushed for 2 h under He and finally cooled down to 35 °C. The samples were evacuated at 25 °C for 2 h under a residual pressure of <5 μmHg. A first H_2 adsorption isotherm was taken at 25 °C. Then the sample was evacuated at the same temperature and a second H_2 adsorption isotherm was measured. The difference between the two isotherms corresponds to the amount of hydrogen chemisorbed on the samples at 25 °C. These values were used to estimate the dispersion assuming a 1:1 ratio between the chemisorbed gas atoms and the active metal atoms (1 H_2 molecule for 2 Rh atoms). Dispersion ((amount of Rh exhibit/amount of total Rh) × 100%) is calculated by the expression: (moles of H_2 adsorbed × 2 × 100%)/(amount in Rh (ICP) × mass of sample).

In situ diffuse reflectance infrared Fourier transform spectroscopy (DRIFTS) experiments were performed to study the evolution of the adsorption of surface species on the catalyst. Spectra were collected on a Bruker Equinox 55 infrared spectrometer equipped with an air cooled laser IR de tyope Globar (MIR) source with KBr optics and a MCT detector. Spectra were obtained using the programme OPUS/IR 2.2 Brucker by collecting 200 scans from 400 to 4300 cm^{-1} with a resolution of 4 cm^{-1} and are presented in absorbance mode without any manipulation. Samples were placed inside a commercial in situ cell (Spectra-Tech 0030-102) with two ZnSe windows. A thermocouple is placed directly in the catalytic bed in order to control the temperature.

Table 1
Catalytic test results. Pulses of CO_2 and CO on Rh(1%)/γ-Al_2O_3.

Experimental conditions Carrier gas/T (°C)/P (kPa)	Methane production (μmol of CH_4/g_{cat}/min)
CO_2	
H_2/100/300	0.135
H_2/125/300	0.167
H_2/200/300	0.280
He/125/300	0
CO	
H_2/125/300	0.152
H_2/140/300	0.287
H_2/150/300	0.315
H_2/175/300	0.480

3. Results

3.1. Catalytic test

Blank test: in the absence of catalysts (glass beads) no reaction occurs. Only H_2 and CO_2 were observed.

3.1.1. Pulses of CO_2

From Table 1, it is observed that the rate of methane formation increases with the temperature. At low pressure, no methane is formed. When H_2 is replaced by He as carrier gas, no formation of methane was observed either.

3.1.2. Pulses of CO

From Table 1, it is observed that the methane formation rate increases significantly when the temperature increases. At low temperatures (100 °C, 125 °C), CO_2 is more active than CO. When temperature is higher (140–175 °C), CO is more active than CO_2.

3.1.3. Pulses of mixtures of CO_2 and CO

Results are presented in Table 2. When the amount of CO in the pulse increases, the reaction rate (μmol of CH_4/g of catalyst/min) increases significantly. When the amount of CO is very low, no formation of methane is observed.

3.1.4. Influence of the presence of oxygen in the feed. Mixtures of CO_2 and O_2 or CO and O_2

Table 3 shows that in the mixtures of CO_2 with O_2 and CO with O_2. In both cases, the reaction rate reaches a maximum as a function of the amount of O_2 introduced in the pulse. Oxygen clearly has a positive effect on the rate of reaction. When the amount of O_2 is low, the rate of methane formation is higher compared to the rate observed in the absence of O_2. However, when the amount of oxygen is too high, the rate decreases, in this case a negative effect on the reaction rate is observed.

3.2. Physico-chemical characterization

3.2.1. ICP and XRD diffraction

The experimental amount of rhodium is similar to the theoretical one (about 1% in weight). The X-ray analysis showed only peaks correspond to gamma alumina [9]. No peaks corresponding to rhodium were observed. The same results were obtained after reduction treatment and after catalytic test.

Table 2
Catalytic test results. Pulses of mixtures of CO_2 and CO (99/1, 90/10 and 80/20, v/v) on Rh(1%)/γ-Al_2O_3.

Experimental conditions Carrier gas/T (°C)/P (kPa)	Methane production (μmol of CH_4/g_{cat}/min)
(99:1)/H_2/125/300	Non measurable
(90:10)/H_2/125/300	0.0455
(80:20)/H_2/150/300	0.103

Table 3
Catalytic test results. Pulses of mixtures of CO_2 and O_2 and CO and O_2 on Rh(1%)/γ-Al_2O_3.

Experimental conditions Carrier gas/T (°C)/P (kPa)	Methane production (μmol of CH_4/g_{cat}/min)
Mixtures $CO_2 + O_2$	
(100:0)/H_2/150/300	0.155
(97:3)/H_2/150/300	0.245
(95:5)/H_2/150/300	0.263
(93:7)/H_2/150/300	0.156
(90:10)/H_2/150/300	0.154
(85:15)/H_2/150/300	0.132
Mixtures $CO + O_2$	
(100:0)/H_2/150/300	0.315
(97:3)/H_2/150/300	0.444
(95:5)/H_2/150/300	0.426
(93:7)/H_2/150/300	0.593
(90:10)/H_2/150/300	0.319

3.2.2. N_2 adsorption

The specific surface area of the support remains practically unchanged after calcination (77 m^2/g). The support is mesoporous. The deposition of rhodium and the reduction treatment lead to weak increases of the pore volume and the pore diameter, with a surface are of 70 m^2/g. After reaction with a pulse of CO_2, a weak decrease on the BET surface area was observed.

3.2.3. Chemisorption of CO_2 and H_2

After treatment in the presence of H_2, a weak amount of CO_2 is adsorbed on the pure support. On the Rh(1%)/Al_2O_3 catalyst, after the same treatment, the amount adsorbed is about 3–4 times greater. The percentage of dispersion of the impregnated rhodium calculated from the amount of chemisorbed H_2 (0.463 cm^3/g) corresponds to 40.1%.

3.2.4. X-ray photoelectron spectroscopy (XPS)

The peak of rhodium has been decomposed in four components forming two doublets. The first doublet corresponds to Rh $3d_{5/2}$ (position ≈ 307.5 eV) and Rh $3d_{3/2}$ (position ≈ 312.2 eV) and are attributed to rhodium under its metallic form. The second doublet corresponds to Rh $3d_{5/2}$ (position ≈ 309.5 eV) and Rh $3d_{3/2}$ (position ≈ 314.2 eV) and is attributed to rhodium under its oxidized form [6,10]. The areas related to these components allow to determine the XPS Rh^0/Rh_{total} atomic ratio. From Table 4, it is observed that the percentages of carbon and rhodium remain unchanged for the different treatments. The XPS O/Al and Rh/Al atomic ratios remain also relatively constant. The XPS O/Al atomic ratio is close to 1.5, which corresponds to the theoretical atomic ratio (Al_2O_3). The XPS Rh^0/Rh_{total} atomic ratio corresponds to 13% for the fresh catalysts and increases to 82% after reduction treatment. After the catalytic test with the pulse of CO_2, the Rh^0/Rh_{total} XPS atomic ratio decreases to 71% indicating that the catalyst is oxidized by CO_2. This oxidation is not observed in the presence of CO.

Table 4
XPS analysis of Rh(1%)/γ-Al_2O_3 catalyst: fresh, after reduction, after a pulse of CO_2.

Sample	%C	%Rh	O/Al	Rh/Al	$\%Rh^0/Rh_{total}$
After synthesis	9.8	0.2	1.68	0.007	13
After reduction at 350 °C (under H_2)	8.3	0.2	1.66	0.006	82
After a pulse of CO_2 at 125 °C	9.0	0.2	1.64	0.007	71

Table 5
XPS analysis of Rh(1%)/γ-Al_2O_3 catalysts after a pulse of mixture of CO_2 and CO with different molar ratios. T = 125 °C.

Sample	%C	%Rh	O/Al	Rh/Al	$\%Rh^0/Rh_{total}$
After pulse CO_2/CO (99/1)	9.3	0.2	1.70	0.006	81
After pulse CO_2/CO (90/10)	8.9	0.2	1.71	0.005	81
After pulse CO_2/CO (80/20)	9.4	0.2	1.64	0.005	82

Table 5 presents the results related to Rh/γ-Al_2O_3 after the tests introducing pulses of mixtures of CO_2 and CO in different proportions (CO_2/CO).

From Table 5, it is observed that the values of the percentage of carbon and rhodium and the XPS O/Al and Rh/Al atomic ratio remain relatively close to those presented in Table 4. In spite of the fact that CO_2 is introduced in a higher proportion in comparison with CO, the catalyst is not oxidized. The Rh^0/Rh_{total} XPS atomic ratio remains the same as after reduction treatment.

Table 6 presents the results observed with Rh/γ-Al_2O_3 after a pulse of mixtures of CO_2 and O_2 in various CO_2/O_2 proportions in volume (97/3, 95/5, 93/7, 90/10 and 85/15). From the table, it is observed that the percentage of carbon and rhodium and the Rh/Al XPS atomic ratio remain unchanged when oxygen is introduced in the pulse. The XPS O/Al atomic ratio decreases slightly after pulses. These values correspond to the values observed in the presence of pure CO_2. Compared to experiments in the presence of pure CO_2, the XPS Rh^0/Rh_{total} atomic ratio remains unchanged.

Table 6 presents the results observed on Rh/γ-Al_2O_3 after test in the presence of mixtures of CO with O_2 with different CO/O_2 proportions. From Table 6, it can be seen that the percentage of carbon and rhodium, as well as the XPS O/Al and Rh/Al atomic ratio remain nearly unchanged when oxygen is introduced in the mixture. The values are of the same order as those observed in Tables 4–6. The percentage of XPS Rh^0/Rh_{total} atomic ratio decreases when oxygen is introduced in the mixture. Clearly O_2 in the reactant atmosphere oxidizes the catalyst.

3.2.5. DRIFTS analysis

The adsorption of CO_2 at 250 °C and the subsequent flushing with He and hydrogenation allow us to verify that the only features changing during reaction are the bands due to CO adsorption which are located at 1800–2200 cm^{-1} (Fig. 1). For that reason, in the following DRIFT spectra it will be shown solely that region.

3.2.5.1. Test with CO_2.

3.2.5.1.1. Adsorption of CO_2. Three peaks are observed during the introductions of CO_2 (Fig. 2). The central peak

Table 6
XPS analysis on Rh(1%)/γ-Al_2O_3 catalyst after a pulse of a mixture of CO_2/O_2 and CO/O_2. Temperature is 125 °C.

Sample	%C	%Rh	O/Al	Rh/Al	$\%Rh^0/Rh_{total}$
$CO_2 + O_2$					
After pulse CO_2/O_2 (100/0)	9.3	0.2	1.77	0.006	71
After pulse CO_2/O_2 (97/3)	8.6	0.2	1.60	0.006	70
After pulse CO_2/O_2 (95/5)	9.2	0.2	1.51	0.005	68
After pulse CO_2/O_2 (93/7)	9.6	0.2	1.52	0.007	68
After pulse CO_2/O_2 (90/10)	9.2	0.2	1.55	0.005	68
After pulse CO_2/O_2 (85/15)	9.5	0.2	1.52	0.005	68
$CO + O_2$					
After pulse of CO/O_2 (100/0)	7.2	0.2	1.68	0.005	82
After pulse of CO/O_2 (97/3)	7.6	0.2	1.57	0.006	78
After pulse of CO/O_2 (95/5)	7.2	0.2	1.54	0.005	77
After pulse of CO/O_2 (93/7)	7.9	0.2	1.52	0.005	78
After pulse of CO/O_2 (90/10)	7.7	0.2	1.78	0.005	77

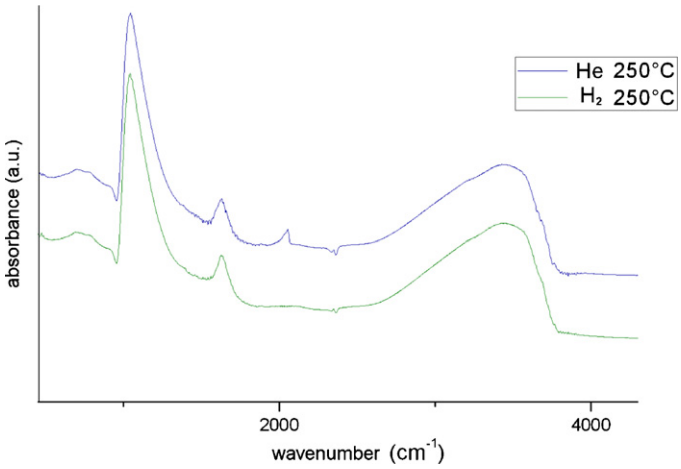

Fig. 1. DRIFT spectra of Rh(1%)/γ-Al_2O_3 after adsorption of CO_2 at 250 °C and subsequent He flushing and hydrogenation.

(2042–2067 cm^{-1}) is attributed to CO adsorbed linearly on rhodium with a zero oxidation state. The two other peaks (2020–2030, antisymmetrical vibration and 2090–2100, symmetrical vibration) are attributed to $Rh(CO)_2$ dicarbonyls adsorbed on rhodium with an oxidation state of +1 [11–18]. The amount adsorbed seems to be stabilized after 30 min.

3.2.5.1.2. Reaction with H_2. After introduction of H_2, the peaks corresponding to gem-dicarbonyls species disappear immediately (Fig. 3). On the contrary, a small peak corresponding to linear CO remains. gem-dicarbonyls species are more reactive than the linear ones.

3.2.5.2. Test with CO.

3.2.5.2.1. Adsorption of CO. The same peaks visible during the introduction of CO_2 are observed (Fig. 4). However in this case, the amount adsorbed remains constant during the adsorption after 30 min. The amount of adsorbed species is higher in the case of CO adsorption compared with the adsorption of CO_2.

3.2.5.2.2. Reaction with H_2. When hydrogen is fed (Fig. 5), the peaks corresponding to gem-dicarbonyls disappear immediately, whereas the peaks corresponding to linear CO start to decrease for increasing later.

3.2.5.3. Tests with CO_2 and CO.

3.2.5.3.1. Adsorption of CO_2 followed by adsorption of CO. Fig. 6 shows two spectra. One spectrum was obtained after CO_2 feeding;

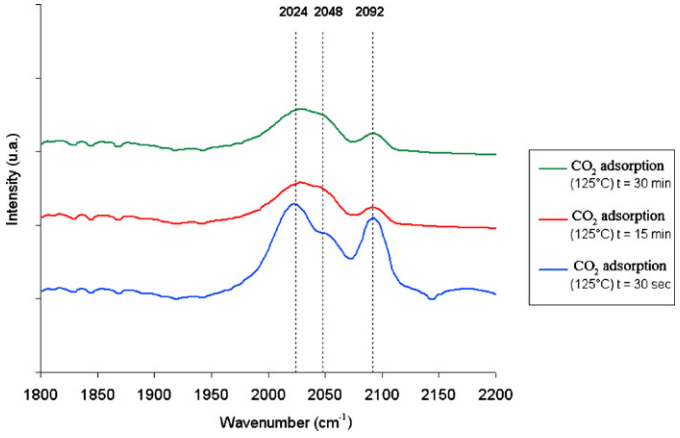

Fig. 2. DRIFTS results after adsorption of CO_2 on Rh(1%)/γ-Al_2O_3 at 125 °C and atmospheric pressure, after 30 s, 15 min and 30 min.

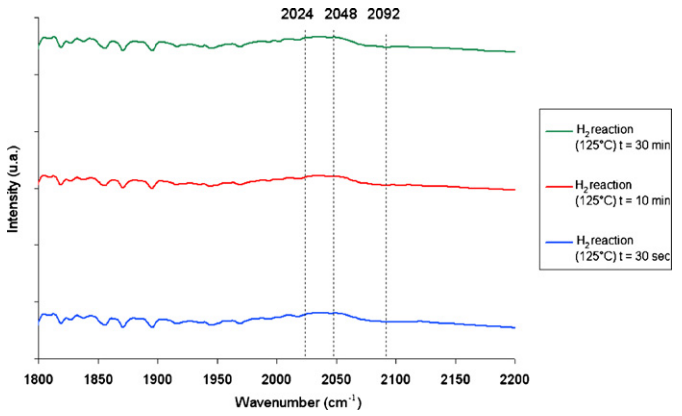

Fig. 3. DRIFTS results after adsorption of CO_2 on Rh(1%)/γ-Al_2O_3 at 125 °C and atmospheric pressure, and after reaction with hydrogen after 30 s, 10 min and 30 min.

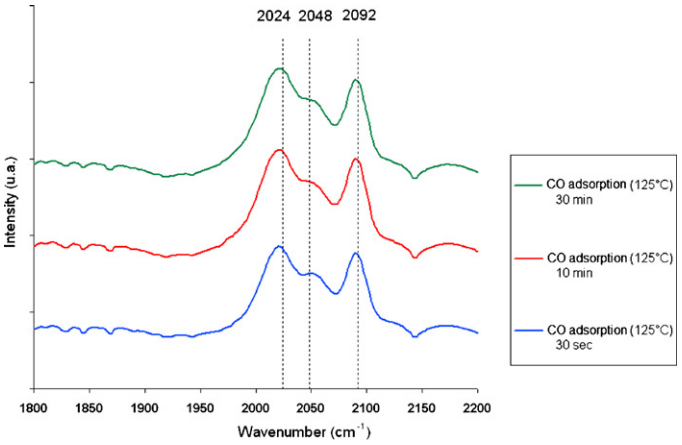

Fig. 4. DRIFTS results after adsorption of CO on Rh(1%)/γ-Al_2O_3 at 125 °C and at atmospheric pressure, after 30 s, 15 min and 30 min.

the other one was obtained after subsequent flushing with He and then introduction of CO. It is observed that during the introduction of CO, the intensity of the adsorption peaks increases, indicating that after adsorption of CO_2 the surface is not saturated with the adsorbed species and CO can still be adsorbed.

3.2.5.3.2. CO adsorption followed by CO_2 adsorption. When the CO is fed and then, after flushing with He, CO_2 is introduced, the intensity of the adsorbed peaks remains unchanged after the adsorption of CO_2 (Fig. 7). During the adsorption of CO, all the

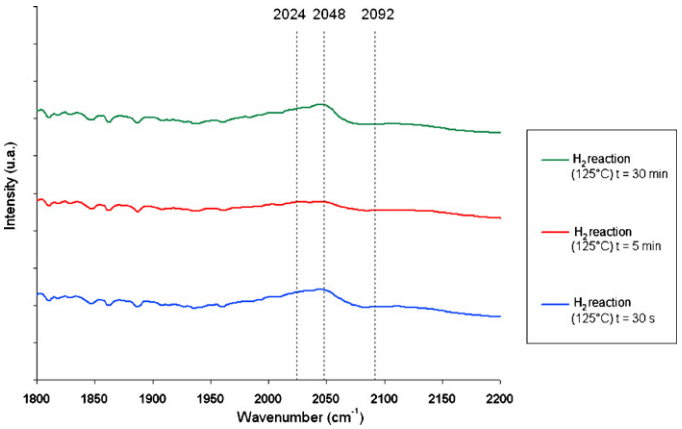

Fig. 5. DRIFTS results after adsorption of CO on Rh(1%)/γ-Al_2O_3 at 125 °C and at atmospheric pressure, and after reaction with hydrogen after 30 s, 5 min and 30 min.

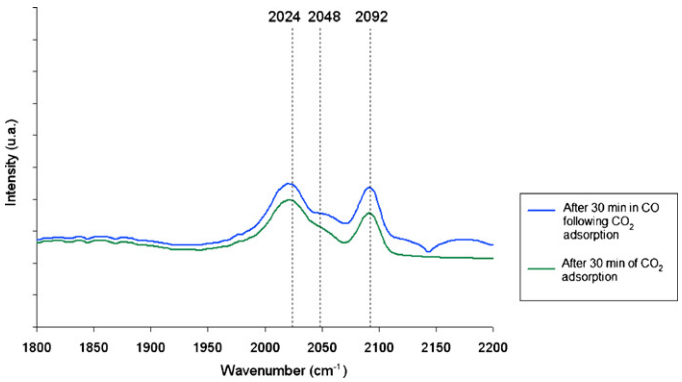

Fig. 6. DRIFTS results for Rh(1%)/γ-Al_2O_3 after adsorption of CO_2 at 125 °C and at atmospheric pressure during 30 min; and after 30 min under a flux of CO, after the adsorption of CO_2.

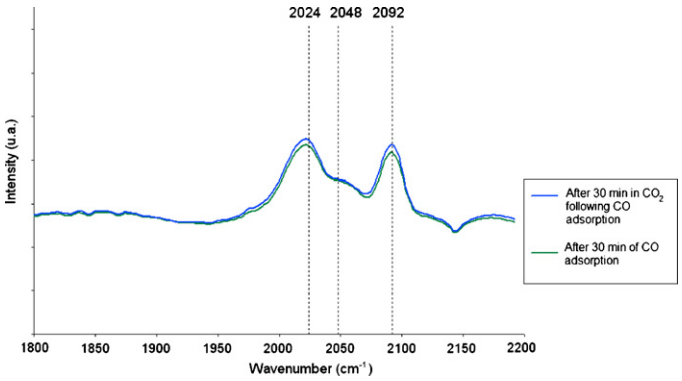

Fig. 7. DRIFTS results for Rh(1%)/γ-Al_2O_3 after adsorption of CO at 125 °C and at atmospheric pressure, after 30 min and under a flux of CO_2, after the adsorption of CO and after 30 min.

sites of adsorption are saturated. CO is more easily adsorbed than CO_2.

3.2.5.4. Test with O_2. The presence of a small amount of O_2 during the adsorption of CO influences the distribution of adsorbed species. In the presence of O_2, the CO gem-dicarbonyl feature decreases in intensity whereas CO linear is completely absent (Fig. 8).

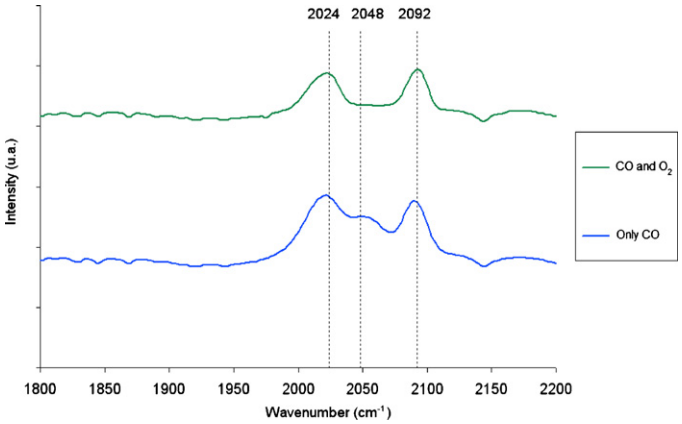

Fig. 8. DRIFTS results after adsorption of pure CO on Rh(1%)/γ-Al_2O_3 at 125 °C and atmospheric pressure after adsorption of CO in the presence of a small amount of O_2

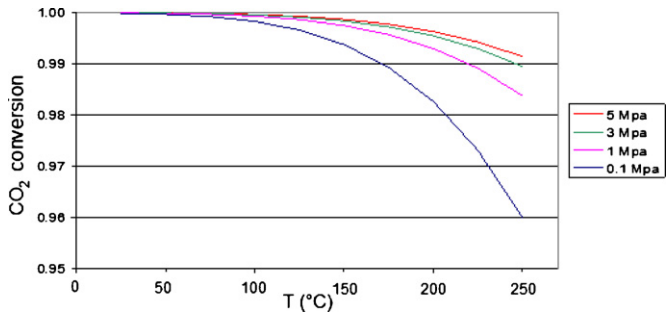

Fig. 9. Equilibrium conversion of CO_2, starting from a stoichiometric mixture (CO_2:H_2:He = 1:4:7).

3.3. Thermodynamic calculations

The equilibrium composition of mixtures that could potentially be obtained by reacting CO_2 and H_2 diluted in He has been calculated from thermodynamic data using the EPIC2 software. The calculation algorithm was based on the minimisation of the Gibbs free energy of the system, constrained by atomic balances [19]. It was assumed that all the molecules containing one or two carbon atoms are likely to be formed. The mixture is considered as an ideal gas and all possible reactions between both reactants are studied. The following components were included in the model: CO_2, H_2, CO, H_2O, He, CH_4, methanol, methanal, acetic acid, methyl acetate, dimethylether, formic acid et methyl formate. In both runs only the first 6 components appeared to be formed in a significant amount in the equilibrium mixture (mole fraction $>10^{-9}$).

Table 7 presents the results obtained in the first run at 25 °C with CO_2 as reactant. Similar results are observed at the other temperatures. In all cases, CO_2 (25% conversion) and H_2 (100% conversion) have reacted to form only methane, the only hydrocarbon molecule which can be formed under equilibrium conditions. As shown in Fig. 9, in the temperature range considered, the conversion of CO_2 is almost complete, even when the initial mixture is in stoichiometric proportions; thus an excess of H_2 is not needed to achieve a high conversion. CO_2 conversion is favoured by a higher pressure, only traces of CO are formed, and the equilibrium selectivity is above 99.99% in all the conditions discussed here. When CO is used as reactant, similar results are observed, except that in this case the conversion of CO is 33%. As in the case of CO_2 hydrogenation, conversion of H_2 is complete and no other hydrocarbon, except of methane, was formed (Table 7).

From the first run calculations it can be concluded that under the experimental conditions used, the only reaction products which can be formed are methane and water. No other chemical compound is thermodynamically expected to be formed. In addition, the methane and water formed correspond to the stoichiometric reaction: $CO_2 + 4H_2 = CH_4 + 2H_2O$. The thermodynamic results are consistent with the experimental results obtained in this work.

In Table 7 are shown the results obtained for the reaction between CO_2 and H_2 in the presence of 1% in volume of CO and the reaction between CO_2 and H_2 in the presence of 1% in volume of O_2. From Table 7, it is observed that the hydrogenation of CO_2 thermodynamically predicted to be possible at 25 °C and atmospheric pressure with 100% selectivity. The presence of CO or O_2 have a negative influence on the amount of methane formed, as in the conversion of CO_2 or CO, however the selectivity remains in both cases unchanged at 100%.

4. Discussion

4.1. Evolution of the catalyst during treatments and after pulses of pure CO_2

XRD analysis confirms that the support of the catalyst is γ-Al_2O_3. In Rh/γ-Al_2O_3 catalyst, rhodium is effectively deposited on the surface of the support (1% in weight and about 2% on the surface). After deposition of rhodium, the increase in the pore size could be due to the deposition of Rh inside the pores of the alumina [6]. After reduction, there is no modification in the textural properties of the catalyst. However, rhodium is effectively reduced. The XPS Rh^0/Rh_{total} atomic ratio increases from 13% to 19% after synthesis to 82% after reduction.

After reaction there is not any textural modification, except slight decreases in the BET surface. However a slight oxidation of the catalysts occurs. The XPS Rh^0/Rh_{total} atomic ratio decreases from 82% to 71% after pulse. The fact that CO_2 is able to oxidize the catalyst surface has been observed in the case of gold by Mihaylov et al. [20].

It is emphasized that this oxidation is not observed after the pulse with CO. In this case, the catalysts remains reduced. The XPS C/Al atomic ratio values, confirms that there is no carbon deposition during the catalytic tests.

4.2. Mechanism of adsorption and of the reaction of CO_2

The adsorption of CO_2 on the catalysts has been proved by chemisorption of CO_2. When Rh is deposited on the alumina, the amount of CO_2 chemisorbed is about 3–4 times more important than that on the pure support. Experimentally it was determined that, at 125 °C under a pressure of 2 bar, about 36% of the amount of CO_2 fed by the pulse is adsorbed on the surface of the catalyst. The amount adsorbed depends on the reaction conditions. These results allows us to confirm that CO_2 is effectively adsorbed on the Rh(1%)/γ-Al_2O_3 catalysts. However these results do not give information on the way how CO_2 is adsorbed. At present, two mechanisms of reaction have been proposed in the literature. The first one suggests the formation of a formiate species as intermediate. CO_2 is activated by Rh, but the formiate is located on the support. These species are decomposed in CO, which is able to react with hydrogen to give methane. The scheme of the reaction would be as follows [21]. Indexes S, M et I refer to support, metal and interface.

$$CO_2 + (OH^-)_S \overset{\text{first}}{\leftrightarrow} (HCO_3^-)_S \overset{+2H_M}{\leftrightarrow} (HCOO^-)_I + H_2O \rightarrow (CO)_M + (OH^-)_S \overset{+6H_M}{\Rightarrow} CH_4 + H_2O$$

$$\updownarrow$$

$$(HCOO^-)_S$$

The second mechanism proposes the dissociation of CO_2 in CO and O adsorbed species. The adsorbed CO would be the intermediate which could react with hydrogen to form methane, without formation of formiate. In both mechanisms the CO would be the intermediate which can be desorbed or react with hydrogen to form methane, after dissociation in C and O monoatomic species. In both mechanisms the intermediate formed is adsorbed CO. The difference is the way how this intermediate is formed.

Studies in literature support both mechanisms [16,22,23], however under the experimental conditions used in this work, two results seem to favour the second mechanism. DRIFTS results obtained with CO_2 and CO showed that the adsorbed species are identical in both cases and in any case was the formation of formate species observed. The methanation reaction of CO_2 will follow the same mechanism as the methanation of CO. The only difference could be the dissociation step of CO_2 which allows promoting the

Table 7
Thermodynamic calculations. Equilibrium concentrations, starting from different mixtures at 25 °C and 100 kPa.

	He	CO_2	CO	O_2	H_2	CH_4
CO_2/H_2/He						
Flow IN (kmol/s)	0.83	0.0833	–	–	0.0833	0
Flow OUT (kmol/s)	0.83	0.0625	–	–	1.61×10^{-6}	0.0208
Conversion (%)	0	25	–	–	100	–
Selectivity (%)	–	–	–	–	–	100
CO/H_2/He						
Flow IN (kmol/s)	0.83	–	0.0833	–	0.0833	0
Flow OUT (kmol/s)	0.83	–	0.0555	–	1.15×10^{-9}	0.0278
Conversion (%)	0	–	33.4	–	100	–
Selectivity (%)	–	–	–	–	–	100
CO_2/H_2/He + 1% CO						
Flow IN (kmol/s)	0.82	0.0833	0.0100	–	0.0833	0
Flow OUT (kmol/s)	0.82	0.0700	0	–	0	0.0233
Conversion (%)	0	16	100	–	100	–
Selectivity (%)	–	–	–	–	–	100
CO_2/H_2/He + 1% O_2						
Flow IN (kmol/s)	0,82	0.0833	–	0.0100	0.0833	0
Flow OUT (kmol/s)	0,82	0.0675	–	0	0	0.0158
Conversion (%)	0	19	–	100	100	–
Selectivity (%)	–	–	–	–	–	100

oxidation of the catalysts. On the other hand, XPS indicates without ambiguity that the catalyst is oxidized after pulse of CO_2. This oxidation does occur only in the presence of pure CO_2. This is a strong indication that CO_2 is dissociated in adsorbed CO and O. The oxygen could be responsible for the oxidation.

4.3. Reactivity of adsorbed species with H_2

The CO adsorbed corresponds essentially to linear-CO and $Rh(CO)_2$ gem-dicarbonyl (DRIFTS). The gem-dicarbonyls species are more reactive than the linear species. This is explained because the Rh–CO bonding in Rh–CO linear is stronger than that in Rh–$(CO)_2$ [11].

Experiments at different temperatures have allowed to calculate the activation energy of the reaction of methanation of CO_2 and CO. Values of 10.7 and 35.4 kJ/mol have been obtained respectively.

Table 8 gives the *E* values for these two reactions as reported in the literature. One can notice that the values of activation energy observed in the present study are lower than those reported in literature. Differences could be explained by the different experimental conditions, in particular the lower temperature used in this work. It could be argued that because the temperature of reaction is lower, probably the influence of the CO_2 dissociation in the mechanisms is more important. The mechanism via formiate formation, as has been claimed in the literature, seems to operate at higher temperature and with higher activation energy. Nevertheless, it is clearly seen that the activation of energy of the methanation of CO is significantly more elevated that that of the methanation of CO_2. The sole difference in these reactions is the dissociation step of CO_2. This step leads to the oxidation of the catalyst (XPS). The DRIFTS experiments indicate that the way by which the adsorption is realized depends on the oxidation state of rhodium. The formation of gem dicarbonyls species is favoured by a higher oxidation state of rhodium, while linear-CO formation is favoured by metallic rhodium. This has also been observed in the literature by DRIFTS analysis, using Rh/Al_2O_3 catalysts under different reducing treatments [11]. Oxidation of catalysts increases the gem dicarbonyls/CO linear ratio, favouring the formation of more reactive species. DRIFTS experiments show unquestionably that in the presence of H_2 gem-dicarbonyls disappear more rapidly than CO linear species. As gem-dicarbonyls species are formed in great proportion, in the range of temperature studied, an increase of the temperature will have only a minor effect on the amount of these species adsorbed on the catalysts, then on the reaction rate and the activation energy will be lower. The contrary will be observed in the case of the methanation of CO, in which the catalyst will not be oxidized.

Table 8
Activation energies (*E*) for CO_2 and CO methanation with H_2 at atmospheric pressure.

Catalyst	Temperature (°C)	*E* (kJ/mol)	Reference
CO_2 methanation			
0.5% Rh/TiO_2	200–300	103	[24]
5% Rh/Al_2O_3	200–275	68	[21]
5% Rh/SiO_2	200–275	72	[21]
1% Rh/TiO_2	200–275	81	[21]
Rh (sheet)	250–400	67	[25]
CO methanation			
Sheet of Rh	250–400	104	[25]
0.5% Rh/Al_2O_3	250	108	[26]

4.4. Influence of the presence of CO and O_2 in the reactive atmosphere containing CO_2

4.4.1. Presence of CO_2

Catalytic tests show that CO inhibits the reaction of methanation. In the case of the mixtures of CO_2 and CO, the methane produced will come principally from the hydrogenation of CO. The test with a mixture consisting of CO_2 and CO in the proportion of 99/1, which does not produce methane, indicates that the inhibition of the methanation of CO_2 by CO is complete. At 125 °C, CO is less reactive than CO_2. DRIFTS confirms this observation. It is clearly established that CO is adsorbed more easily than CO_2 and that the adsorbed peak in the case of CO_2 (mainly gem-dicarbonyls species) disappear immediately.

4.4.2. Presence of O_2

The tests indicate that O_2 could have a positive effect on the methanation of CO_2. Oxygen in low proportion improves performances. Nevertheless, if the amount of O_2 is too high, a negative effect is observed. The same effects are observed in the case of CO and O_2. Fig. 10 presents the methane produced as a function of the CO_2/O_2 molar ratio. Theoretical values are also presented. These values correspond to the methane which has to be produced taking into account the real amount of CO_2 introduced in the reactor. If the experimental value is higher than the theoretical one, it can be concluded that O_2 has a positive effect. Clearly a maximum depending on the amount of O_2 fed to the reactor is observed. Fig. 11 presents the methane produced as a function of the CO/O_2

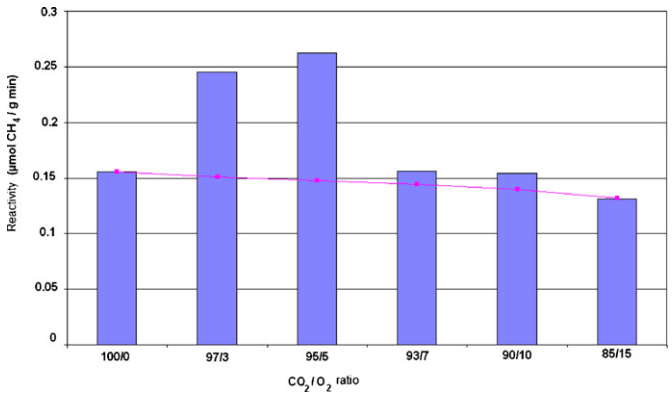

Fig. 10. Amount of methane produced (µmole of methane by gram of catalyst/minute) as a function of the CO_2/O_2 ratio over Rh(1%)/γ-Al_2O_3 at 125 °C. Theoretical values are also given.

molar ratio. Results observed for $CO_2 + O_2$ and $CO + O_2$ mixtures are similar.

XPS analysis shows that the oxygen in low amount is able to oxidize rhodium. The same results have been observed for mixtures of O_2 with CO_2 and CO. The positive effect can be explained by the fact that oxygen favours the oxidation and consequently the formation of the more reactive species. DRIFTS experiments in the presence and absence of O_2 confirm this explanation. Oxygen favours the formation of gem-dicarbonyl. It is important to establish that, comparing mixtures of CO_2 and CO with O_2, the positive effect of oxygen, in the case of mixtures of CO, is maintained for higher amounts of oxygen. The explanation lies in the fact that, in the case of CO_2, it is necessary to consider also the oxidation of rhodium by the adsorbed oxygen resulting from the dissociation of CO_2. The negative effect could be explained by a deep oxidation of the catalysts. However, XPS results show that after a certain proportion of O_2, the catalyst is not oxidized anymore. The second alternative is a competition between CO and O_2 for the adsorption sites. Unfortunately, we have not obtained in the literature results showing the effect of O_2 in methanation which could allow us to compare our results with previous ones. These results seem to be of a great originality with important implications in methanation process.

4.5. Comparison with thermodynamic predictions

It is important to establish that the trends predicted by thermodynamics are confirmed by the experimentation. The selectivity in the formation of methane from CO_2 and CO is 100%. The conversion is higher for the methanation of CO. When CO_2 is fed with a small amount of CO, the reaction of methanation of CO seems to be favoured. The presence of CO has an inhibitor effect on the methanation of CO_2. However, the tendency predicted by thermodynamics is different when a small amount of oxygen is introduced in the feed. Thermodynamics indicates an inhibitor effect of oxygen; on the contrary, a positive effect is observed experimentally when a small amount of oxygen is fed. This difference could be explained by a modification of the kinetics of the reaction due to the presence of the catalysts. However, it is important to underline that in both cases, the selectivity in the formation of methane is 100%.

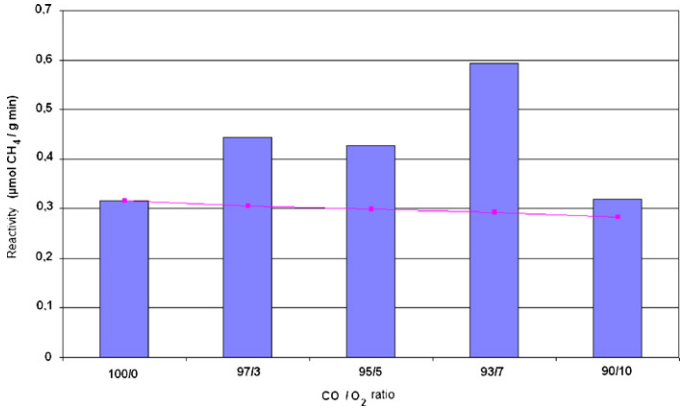

Fig. 11. Amount of methane produced (µmole of methane by gram of catalyst/minute) as a function of the CO/O_2 ratio. Rh(1%)/γ-Al_2O_3 at 125 °C. Theoretical values are also given.

4.6. Outlooks

The present results open new perspectives for the use of CO_2. Presently, CO_2 is investigated as an oxidant at high temperature (>500 °C) in the catalytic oxidation of hydrocarbons to produce chemicals [1,2]. The principal criticism of these processes is the high energy consumption. Our results suggest that the use of the dissociative chemisorption of CO_2 could probably allow to decrease such reaction temperatures and, in addition, to activate other hydrocarbons.

In the light of the present results, it seems that the methanation of CO_2 at low temperature could be a realistic solution for the control of increasing emissions of CO_2, in spite of the fact that more research should be carried out in order to reach the optimal reaction conditions to improve the catalytic performances (temperature, pressure, nature of the catalyst, catalysts promoter, etc.). It is interesting to underline that presently catalysts with an activity in the formation of methane 10 times higher that the values present in this work, maintaining the selectivity as high as 100% working at low temperature (125 °C), have been synthesized using different supports (work in progress). Fundamental research could certainly allow the development of the process of low temperature methanation at an industrial level. Present solutions used to reduce emissions of CO_2, like the underground storage of important volumes of CO_2 could be replaced, in a large part, by methanation at low temperature. The principal criticism of the recycling of CO_2 process could be the high amount of hydrogen which is necessary for the methanation step. However, many industries do produce an excess of hydrogen and on the other hand, hydrogen can be produced by water electrolysis. The corresponding electric energy could be furnished by means of "green" processes: solar cell panels, wind, biomass, etc. It can be argued that, at present, this process is probably too expensive to be industrialised, but it is clear that a deeper knowledge of the main parameters from which methane formation depends will allow to reduce the costs and to perform the process in economical conditions. This and the sustainable character of the process seem to constitute a realistic solution for the reduction of CO_2 emissions. A similar process for recycling the CO_2, as proposed in this work, has been suggested [27,28], however in this process methane is produced at too high temperature (300–400 °C) and it is suggested to burn the produced methane. This is not the more adequate process. Methane produced by this technology has to be injected in the petrochemical and chemical industry, where methane is nowadays used as raw material (oxidation, chlorination, etc.).

A more intelligent way to control emissions could be suggested in the future. Industry could be obliged to recycle a fraction of the CO_2 produced. Higher is the CO_2 recycled, less the industry will be penalized to pay taxes.

Finally, in addition to converting CO_2 in a molecule of high added value, the process of recycling presents the advantage to convert hydrogen in a more easily exploitable source of energy, as is CH_4. In fact, the direct use of H_2 requires specific and expensive infrastructures, a high energetic consumption for its liquefaction; the process

involves transportation and safety difficulties, etc. The possibility to transform H_2 and CO_2 into CH_4 becomes a real alternative as far as environmental protection and security are concerned.

5. Conclusion

The methanation of CO_2 is performed with 100% of selectivity on $Rh/\gamma\text{-}Al_2O_3$ catalyst. Results are coherent with thermodynamic calculations. The amount of methane produced depends on the temperature, pressure, presence or absence of gas promoters, like CO or O_2, in the feed. The only difference in the mechanism of methanation of CO_2 and CO is the dissociation step of CO_2. This dissociation of CO_2 seems to be responsible for the oxidation of the Rh catalysts. The oxidation state of the Rh plays an important role in the distribution of the adsorbed species on the catalysts: the gem-dicarbonyls species are the more reactive ones. The preferential formation of these species will be at the origin of the difference in the reactivity of CO_2 and CO. Oxygen, in low amount, has a positive effect in the methanation. CO inhibits the methanation of CO_2. These results open new prospects of application in catalysis for the recycling of CO_2 in the presence of H_2 as a real alternative for the environmental protection.

Acknowledgements

The authors thank M.J. Genet for his fruitful advices about XPS technique. The authors gratefully acknowledge the “Direction Générale des Technologies, de la Recherche et de l’Energie (DGTRE)” of the “Région Wallonne” (Belgium) and the “Fonds National de la Recherche Scientifique (FNRS)” of Belgium, for their financial support. The involvement of Unité de catalyse et de chimie des matériaux divisés (IMCN, MOST) in the «INANOMAT» IUAP network sustained by the «Service public fédéral de programmation politique scientifique» (Belgium) is acknowledged. AK thanks the “BecasChile” program of Conicyt (Chile) for his research grant. MJ and CS are grateful to the FRIA (Belgium) for their PhD student positions.

References

[1] T. Inui, Catal. Today 29 (1996) 329–337.
[2] C. Song, Catal. Today 115 (2006) 2–32.
[3] I. Gaus, Int. J. Greenh. Gas Con. 4 (2010) 73–89.
[4] S. Bachu, D. Bonijoly, J. Bradshaw, R. Burruss, S. Holloway, N.P. Christensen, O.M. Mathiassen, Int. J. Greenh. Gas Con. 1 (2007) 430–443.
[5] Ruiz, M. Jacquemin, N. Blangenois, WO/2010/006386 (2010).
[6] M. Jacquemin, A. Beuls, P. Ruiz, Catal. Today 157 (2010) 462–466.
[7] G.C. Chinchen, M.S. Spencer, K.C. Waugh, D. Whan, J. Chem. Soc., Faraday Trans. 1 83 (1987) 2193–2212.
[8] L.H. Dubois, G.A. Somorjai, Surf. Sci. 128 (1983) L231–L235.
[9] JCPDFWIN, JCPDS-International Center for Diffraction Data, V. 2.02., 1999.
[10] J.F. Moulder, W.F. Stickle, P.E. Sobol, K.D. Bomben, in: J. Chastain (Ed.), Handbook of X-ray Photoelectron Spectroscopy, 5th ed., Perkin-Elmer Co., Eden Prairie, 1992, p. 72.
[11] D. Duprez, J. Barrault, C. Geron, Appl. Catal. A: Gen. 37 (1988) 105–114.
[12] M.W. Balakos, S.S.C. Chuang, G. Srinivas, M.A. Brundage, J. Catal. 157 (1995) 51–65.
[13] D. Demri, J.P. Hindermann, A. Kiennemann, C. Mazzocchia, Catal. Lett. 23 (1994) 227–236.
[14] Z. Tian, O. Dewaele, G.B. Marin, Catal. Lett. 57 (1999) 9–17.
[15] A.M. Efstathiou, T. Chafik, D. Bianchi, C.O. Bennett, J. Catal. 147 (1994) 24–37.
[16] K. Walter, O.V. Buyevskaya, D. Wolf, M. Baerns, Catal. Lett. 29 (1994) 261–270.
[17] O.V. Buyevskaya, K. Walter, D. Wolf, M. Baerns, Catal. Lett. 38 (1996) 81–88.
[18] Z. Zhang, A. Kladi, X.E. Verykios, J. Catal. 156 (1995) 37–50.
[19] W.B. White, S.M. Johnson, G.B. Dantzig, J. Chem. Phys. 28 (1958) 751–753.
[20] M. Mihaylov, E. Ivanova, Y. Hao, K. Hadjiivanov, B.C. Gates, H. Knözinger, Chem. Commun. (2008) 175–177.
[21] F. Solymosi, A. Erdöhelyi, T. Bansagi, J. Catal. 68 (1981) 371–382.
[22] M. Marwood, PhD Thesis, Ecole Polytechnique de Lausanne, 1994.
[23] G. Weatherbee, C. Bartholomew, J. Catal. 77 (1982) 460–472.
[24] Z. Zhang, A. Kladi, X.E. Verykios, J. Catal. 148 (1994) 737–747.
[25] B. Sexton, G. Somorjai, J. Catal. 46 (1977) 167–189.
[26] P. Panagiotopoulou, D. Kondarides, X. Verykios, Appl. Catal. A: Gen. 344 (2008) 45–54.
[27] K. Hashimoto, M. Yamasaki, K. Fujimura, T. Matsui, K. Izumiya, M. Komori, A.A. El-Moneim, E. Akiyama, H. Habazaki, N. Kumagai, A. Kawashima, K. Asami, Mater. Sci. Eng. A 267 (1999) 200–206.
[28] K. Hashimoto, M. Yamasaki, S. Meguro, T. Sasaki, H. Katagiri, K. Izumiya, N. Kumagai, H. Habazaki, E. Akiyama, K. Asami, Corros. Sci. 44 (2002) 371–386.